Computer Modeling in Engineering & Sciences
DOI:10.32604/cmes.2020.012792
Article

Tech Science Press

Modelling the Effect of Self-Immunity and the Impacts of Asymptomatic and Symptomatic Individuals on COVID-19 Outbreak

M. H. A. Biswas[1,*], M. A. Islam[1], S. Akter[2], S. Mandal[2], M. S. Khatun[1], S. A. Samad[1], A. K. Paul[1] and M. R. Khatun[1]

[1]Mathematics Discipline, Science Engineering and Technology School, Khulna University, Khulna, 9208, Bangladesh
[2]Department of Mathematics, Bangabandhu Sheikh Mujibur Rahman Science and Technology University, Gopalganj, 8100, Bangladesh
*Corresponding Author: M. H. A. Biswas. Email: mhabiswas@yahoo.com
Received: 12 July 2020; Accepted: 16 November 2020

Abstract: COVID-19 is one of the most highly infectious diseases ever emerged and caused by newly discovered severe acute respiratory syndrome coronavirus 2 (SARS-CoV-2). It has already led the entire world to health and economic crisis. It has invaded the whole universe all most every way. The present study demonstrates with a nine mutually exclusive compartmental model on transmission dynamics of this pandemic disease (COVID-19), with special focus on the transmissibility of symptomatic and asymptomatic infection from susceptible individuals. Herein, the compartmental model has been investigated with mathematical analysis and computer simulations in order to understand the dynamics of COVID-19 transmission. Initially, mathematical analysis of the model has been carried out in broadly by illustrating some well-known methods including exactness, equilibrium and stability analysis in terms of basic reproduction number. We investigate the sensitivity of the model with respect to the variation of the parameters' values. Furthermore, computer simulations are performed to illustrate the results. Our analysis reveals that the death rate from coronavirus disease increases as the infection rate increases, whereas infection rate extensively decreases with the increase of quarantined individuals. The quarantined individuals also lead to increase the concentration of recovered individuals. However, the infection rate of COVID-19 increases more surprisingly as the rate of asymptomatic individuals increases than that of the symptomatic individuals. Moreover, the infection rate decreases significantly due to increase of self-immunity rate.

Keywords: COVID-19; asymptomatic and symptomatic individuals; self-immunity; mathematical model; basic reproductive ratio; numerical simulations

1 Introduction

In the earth, viruses are the old detected human killer and in different times the world had to face a big challenge to fight against world pandemic diseases causing a huge loss of life and wealth. Different pandemic situations occurred in several parts of the world over the years [1]. COVID-19 is the most recent emerged devastating fatal disease, caused by coronavirus to make the jump to human infection [2]. However, there are several coronaviruses known to be circulating in different animal population that have not yet been infected human. Middle East Respiratory Syndrome (MERS-CoV) and Severe Acute Respiratory Syndrome (SERS-CoV-2) are the two zoonotic (transmits from animals to humans) corona viruses' outbreaks which have recently been experienced in the world. Coronaviruses are such type of deadly viruses that cause illness ranging from the common cold to severe respiratory disease. The genome of coronavirus is fully sequenced. The genomic sequence of SARS CoV-2 showed identical, but distinct genome composition of SARS-CoV and MERS-CoV. Since its first case reported in late 2019, the infection has spread to other regions in China and other countries, and the transmission rate, the mortality rate and the clinical manifestation slowly emerged [3].

Mathematical modelling is playing a significant role to describe the epidemiology of infectious diseases [4]. Mathematical modelling aims at the mathematical representation of various biological processes such as wound healing, morphogenesis, blood-cell production and dynamics of infectious diseases, using techniques and tools of applied mathematics [5,6]. There exist a number of models for infectious diseases as well as chronic diseases; as for compartmental models and optimal control problem, starting from the very classical SIR model to more complex proposals [7–9]. The classical SIR type compartmental model was first introduced by Kermack and McKendrick in 1927 [10]. Since coronavirus is a zoonotic virus, it first transmits from animals to humans. Once people become infected, then it spreads from human to human by the physical contact with infected human owing to its tremendous infectiousness. So the dynamics of COVID-19 can be described by SIR type epidemic model. It is sometimes more realistic to study such epidemic disease in terms of SEIR model when there is a certain incubation period before showing the symptom. This global outbreak has attracted the interest of researchers of different areas. Several researches of COVID-19 have been carried out focusing on mathematical modelling of the mysterious mechanisms of this disease [11,12]. An estimation of the reproductive number of coronavirus by using simulation has been introduced in [13]. Mathematical modelling of COVID-19 transmission dynamics in Wuhan has been described with stability analysis in [14]. Evolution of the novel coronavirus from the ongoing Wuhan outbreak is discussed in [15]. Aguilar et al. [16] investigate the impact of asymptomatic carriers on COVID-19 transmission. However, some articles [17–27] are referred for more details on SIR and SEIR type analysis and development of mathematical model on the dynamics of COVID-19.

COVID-19 transmission now becomes a worldwide pandemic. Our main contribution in this study is to consider the symptomatic and asymptomatic individuals who have remarkable influenced on the spread of COVID-19. In this paper, we have developed a mathematical model to study the dynamics of the deadly coronavirus disease in terms of nine ordinary nonlinear coupled equations. We have considered rates of change for susceptible, exposed, quarantined, symptomatic, asymptomatic, infected, hospitalized, death as well as recovered individuals. In our study, we have determined the basic reproduction number and studied the existence of the solution of the model with stability or instability criteria at disease-free and endemic equilibrium points. We have also performed sensitivity analysis of the model. Finally, numerical simulations have been performed to show the dynamic behavior of COVID-19.

2 Present Scenario of COVID-19

The novel coronavirus disease (COVID-19) emerged in December 2019 in Wuhan, China and since then it has spread globally resulting in an ongoing pandemic [28]. On 10 July, 2020 in China more than 83,500 cases have been reported and more than 4634 death. Worldwide this scenario is tremendous, more than 12.72 million cases have been reported across 213 countries and territories, ensuing in more than 564,661 death and more than 7.4 million people have recovered [29]. Among them more than 4,738,570 are active case and more than 7,982,416 are closed cases. In active case, 99% is in mid condition and 1% is in serious condition and in closed case, 93% is recovered and 7% is death [30]. After breaking out the COVID-19 in China, Europe is the first continent to suffer severally. Especially in Italy, the situation was more serious and devastating with more than 300,988 infected and more than 28,400 deaths till July 10, 2020 and in Europe more than 2.38 million people were infected and more than 190063 deaths [31].

After Europe, the COVID-19 spread out in American continent being USA as the epicenter in North America followed by Brazil in Latin America. In North America the infected, recovered and death are more than 3.49 million, 1.57 million and 1.75 lakhs respectively and in South America the infected, recovered and death are more than 2.72 million, 1.79 million and 1.049 lakhs as on 10 July, 2020 [32]. India and Bangladesh are in the top most position in COVID-19 infections in Asian continent. According to World Health Organization, Asia is within the foremost risk position within the world of COVID-19 transmission including more than 1.37 million infected, 84.36 lakhs recovered and 35,745 deaths till July 10, 2020 [33]. The second leading infected continent is Africa, having more than 5.59 lakhs infected, 1,93,481 recovered, and 12,769 deaths [34]. The pandemic situation in Australia and Oceania is lowest under control including infected more than 9,553 and 11,834, deaths 107 and 118 respectively [35]. The statistics of global pandemic situation of COVID-19 outbreaks is studied graphically by drawing bar diagram which is presented in Fig. 1.

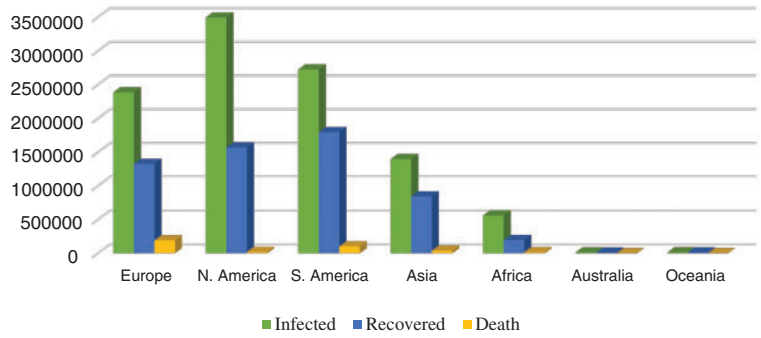

Figure 1: Continent wise total infected, deaths and recovered as on June, 07, 2020 (Source: [32–35])

The age and gender have great influence on COVID-19 infection and deaths. Research shows that the older people are most likely vulnerable to get infected by coronavirus and deaths [30]. Mortality rates are significantly higher at the age of 80 years above and about 14.8%. The worldwide death report in respect to age distribution is given in Fig. 2.

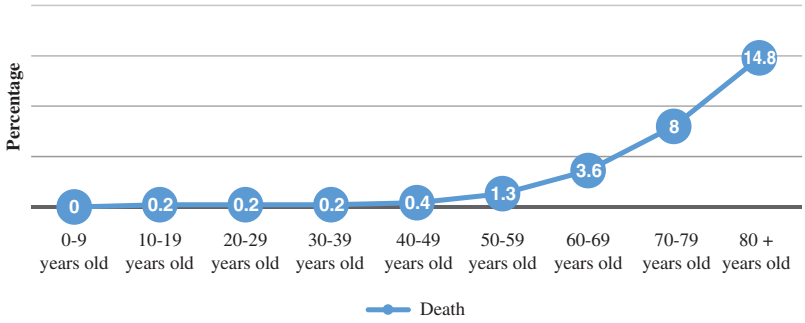

Figure 2: Worldwide age distribution of death rate (Source: [30])

3 Basic Assumption and Formulation of the Model

Coronavirus is primarily spread during close contact via small droplets produced by coughing, sneezing, or talking. The transmission dynamics of COVID-19 occurs when a person is in close contact (within 1 m) with someone who has already infected [27]. Any individual may also become infected by touching a contaminated surface and then touching their face. It is most contagious during the first three days after the onset of symptoms, although spread hours or days may be possible before symptoms appear and in later stages of the disease. However, evidence to date suggests that older people (over 60 years old) and those are already affected by diabetes, chronic respiratory disease and cancer are at a higher risk to be infected by coronavirus. World Health Organization (WHO) has issued advice for these two groups and for community support to ensure that they are protected from COVID-19 without being isolated, stigmatized, left in a position of increased vulnerability or unable to access basic provisions and social care.

So, the whole dynamics of MERS and SARS-CoV-2 (COVID-19) can be described by a SEIR type infectious disease model in terms of a set of nonlinear ordinary differential equations (ODEs). In this paper, we extend the basic SEIR model to nine compartments to show the individual significance of each compartment. We consider quarantine, symptomatic, asymptomatic, hospitalized (or Isolation) and death compartments. The susceptible $S(t)$, who can acquire the infection; exposed $E(t)$, when the virus exposed itself into human bodies; the separation of a person or group of people reasonably believed to have been exposed to a communicable disease, such type of populations are considered as a quarantined populations in this model and these populations are represented by $Q(t)$. The populations who are pertaining to a symptom or symptoms of the COVID-19 disease are considered as symptomatic populations ($M(t)$). The populations presenting no symptoms of the disease, we consider as asymptomatic populations and denoted by $A(t)$. The novel coronavirus can transmit through direct contact with infected people or with objects used on the infected person. Thus the population, who can transmit infection to susceptible, is defined as infected $I(t)$ populations. Since, there is no vaccine and no specific antiviral medicines for COVID-19, those with serious illness, may need to be hospitalized so that they can receive life-saving treatment for complications. In our model, we consider such kind of people as the hospitalized populations presented by $H(t)$. The recovered class $R(t)$ are those who are immunized from infection. Finally, the populations who have died of the COVID-19 are considered as death compartment and denoted by $D(t)$. Let, $N(t)$ be the total population at time t where,

$$N(t) = S(t) + E(t) + Q(t) + M(t) + A(t) + I(t) + H(t) + R(t) + D(t).$$

The transmission mechanisms of the novel coronavirus disease COVID-19 are shown in Fig. 3.

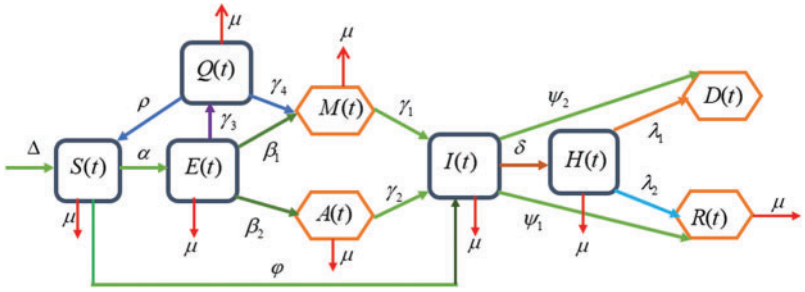

Figure 3: The schematic diagram of the transmission mechanisms of the novel coronavirus disease COVID-19

Taking the above diagram presented in Fig. 3 into consideration, we formulate a nine compartmental model in terms of a set of nonlinear ordinary differential equations (ODEs) of the following form:

$$\frac{dS}{dt} = \Delta + \rho S(t) Q(t) - (\alpha E(t) + \varphi I(t)) S(t) - \mu S(t)$$

$$\frac{dE}{dt} = \alpha S(t) E(t) - (\beta_1 + \beta_2 + \gamma_3) E(t) - \mu E(t)$$

$$\frac{dQ}{dt} = \gamma_3 E(t) - \rho S(t) Q(t) - \gamma_4 Q(t) - \mu Q(t)$$

$$\frac{dM}{dt} = \beta_1 E(t) + \gamma_4 Q(t) - \gamma_1 M(t) - \mu M(t)$$

$$\frac{dA}{dt} = \beta_2 E(t) - \gamma_2 A(t) - \mu A(t) \tag{1}$$

$$\frac{dI}{dt} = \gamma_1 M(t) + \gamma_2 A(t) + \varphi S(t) I(t) - (\delta + \psi_1 + \psi_2) I(t) - \mu I(t)$$

$$\frac{dH}{dt} = \delta I(t) - \lambda_1 H(t) - \lambda_2 H(t) - \mu H(t)$$

$$\frac{dR}{dt} = \lambda_2 H(t) + \psi_1 I(t) - \mu R(t)$$

$$\frac{dD}{dt} = \lambda_1 H(t) + \psi_2 I(t)$$

with initial conditions,

$$S(0) = S_0, \quad E(0) = E_0, \quad Q(0) = Q_0, \quad M(0) = M_0, \quad A(t) = A_0, \quad I(0) = I_0, \quad H(0) = H_0,$$
$$R(0) = R_0 \quad \text{and} \quad D(0) = D_0$$

In the model (1), we have considered the parameter Δ as the recruitment rate of susceptible individuals and α as the exposed rate of the individuals. β_1 and β_2 are the rate at which the symptomatic and asymptomatic individuals becoming infected. The probabilities of transmission of infections from symptomatic, asymptomatic and susceptible individuals are represented by the parameters γ_1, γ_2 and φ respectively. In order to maintain physical distancing, some exposed individuals go to self-quarantined and this rate is represented by the parameter γ_3. Quarantined individuals are divided into parts when they get tested. If these individuals show negative result of infection, they become infection free and hence they again enter into the susceptible individual compartment at a rate ρ. On the other hand, if they express positive result of infection, they enter into the symptomatic individual compartment at rate γ_4. The infected individuals get hospitalized at rate δ. A portion of hospitalized individuals become dead because of the severity of the infection and this phenomenon is denoted by rate λ_1. Another portion of hospitalized individuals get recovered at rate λ_2. Besides, individuals also get recovered due to their strong immunity system and this rate is represented by the parameter ψ_1. Before getting into hospitalization, infected individuals are died at rate ψ_2. Finally, μ denotes the natural death rate of each individual.

4 Mathematical Analysis of COVID-19 Model

In this section, we discuss the boundedness, Positivity, equilibrium analysis, dynamical behavior of those points, local and global stability of the model (1).

4.1 Boundedness of the Model

Theorem 1: The region $\Phi = \left\{(S(t), E(t), Q(t), M(t), A(t), I(t), H(t), R(t), D(t)) \in \mathbb{R}_+^9\right\}$ is a positively invariant set of the proposed model.

Proof: Let the total population size is $N(t)$ where, $N(t) = S(t) + E(t) + Q(t) + M(t) + A(t) + I(t) + H(t) + R(t) + D(t)$.

Then, the growth rate of the total population is $\frac{dN}{dt} = \frac{dS}{dt} + \frac{dE}{dt} + \frac{dQ}{dt} + \frac{dM}{dt} + \frac{dA}{dt} + \frac{dI}{dt} + \frac{dH}{dt} + \frac{dR}{dt} + \frac{dD}{dt}$.

$$\begin{aligned}\Rightarrow \frac{dN}{dt} &= \Delta + \rho S(t) Q(t) - (\alpha E(t) + \varphi I(t)) S(t) - \mu S(t) + \alpha S(t) E(t) - (\beta_1 + \beta_2 + \gamma_3) E(t) \\ &\quad - \mu E(t) + \gamma_3 E(t) - \rho S(t) Q(t) - \gamma_4 Q(t) - \mu Q(t) + \beta_1 E(t) + \gamma_4 Q(t) - \gamma_1 M(t) - \mu M(t) \\ &\quad + \beta_2 E(t) - \gamma_2 A(t) - \mu A(t) + \gamma_1 M(t) + \gamma_2 A(t) + \varphi S(t) I(t) - (\delta + \psi_1 + \psi_2) I(t) - \mu I(t) \\ &\quad + \delta I(t) - \lambda_1 H(t) - \lambda_2 H(t) - \mu H(t) + \lambda_2 H(t) + \psi_1 I(t) - \mu R(t) + \lambda_1 H(t) + \psi_2 I(t)\end{aligned}$$

$$\Rightarrow \frac{dN}{dt} = \Delta - \mu (S(t) + E(t) + Q(t) + M(t) + A(t) + I(t) + H(t) + R(t))$$

$$\Rightarrow \frac{dN}{dt} = \Delta - \mu N$$

After solving the above equation, we have

$$N(t) = \frac{\Delta}{\mu} + \left(N_0 - \frac{\Delta}{\mu}\right) e^{-\mu t}.$$

Therefore, $\lim_{t\to\infty} N(t) = \frac{\Delta}{\mu}$ which indicates that $N_0 \leq \frac{\Delta}{\mu}$ i.e., $\frac{\Delta}{\mu}$ is the upper bound of $N(t)$. On the other hand, if $N_0 > \frac{\Delta}{\mu}$, then $N(t)$ will decrease to $\frac{\Delta}{\mu}$ as $t \to \infty$ i.e., the solutions $(S(t), E(t), Q(t), M(t), A(t), I(t), H(t), R(t))$ approaches the region Φ asymptotically. Therefore, the model is mathematically and epidemiologically well-posed in the region Φ. Hence, the Theorem 1 is proved.

4.2 *Positivity of the Model*

Here, we will show that all the variables in the model (1) are positive.

Theorem 2: If $S(0) \geq 0$, $E(0) \geq 0$, $Q(0) \geq 0$, $M(0) \geq 0$, $A(0) \geq 0$, $I(0) \geq 0$, $H(0) \geq 0$, $R(0) \geq 0$ and $D(0) \geq 0$, then the solutions of the system are non-negative.

Proof: To prove Theorem 2 for the transmission of COVID-19, we recall the first equation of model (1),

$$\frac{dS}{dt} = \Delta + \rho S(t) Q(t) - (\alpha E(t) + \varphi I(t)) S(t) - \mu S(t) \tag{2}$$

In order to find the positivity of the Eq. (2), we can write

$$\Rightarrow \frac{dS}{dt} \geq \Delta - \mu S(t)$$

$$\Rightarrow \frac{dS}{dt} + \mu S(t) \geq \Delta \tag{3}$$

Integrating Eq. (3), we have

$$S(t) \geq \frac{\Delta}{\mu} + c e^{-\mu t}, \quad \text{where } c \text{ is an integrating constant.} \tag{4}$$

We apply the initial condition at $t = 0$, then $S(0) - \frac{\Delta}{\mu} \geq c$. Then putting the value of c, Eq. (4) becomes $S(t) \geq \frac{\Delta}{\mu} + \left(S(0) - \frac{\Delta}{\mu}\right) e^{-\mu t}$. Hence, $S(t) \geq 0$ at $t = 0$ and $t \to \infty$. Therefore, $S(t) \geq 0$ is positive for all $t \geq 0$. Similarly, with the help of [5,9], we obtain $E(t) \geq 0$, $M(t) \geq 0$, $Q(t) \geq 0$, $A(t) \geq 0$, $I(t) \geq 0$, $H(t) \geq 0$ and $R(t) \geq 0$ for all $t \geq 0$.

Hence the Theorem 2 is proved.

4.3 *Disease Free Equilibrium (DFE) Point*

For the disease-free equilibrium point of the model (1), we have to solve

$$\frac{dS}{dt} = \frac{dE}{dt} = \frac{dQ}{dt} = \frac{dM}{dt} = \frac{dA}{dt} = \frac{dI}{dt} = \frac{dH}{dt} = \frac{dR}{dt} = \frac{dD}{dt} = 0 \tag{5}$$

In case of disease free, all the state variables are zero except the susceptible individuals. By solving the system (5), we obtain

$$\Delta + \rho S(t) Q(t) - (\alpha E(t) + \varphi I(t)) S(t) - \mu S(t) = 0$$

$$\Rightarrow S_0 = \frac{\Delta}{\mu}$$

Hence, the disease-free equilibrium point (DFE) of COVID-19 model is $\left(\frac{\Delta}{\mu}, 0, 0, 0, 0, 0, 0, 0, 0\right)$.

4.4 Basic Reproductive Ratio

An important measure of transmissibility of the disease is the epidemiological concept of basic reproductive ratio. It provides an invasion criterion for the initial spread of the virus in a susceptible population.

Definition 4.1: (See [4]) The basic reproduction number, denoted by R_0 is defined as the average number of secondary infections that occurs when one infective is introduced into a completely susceptible population.

4.4.1 Basic Reproduction Number at DFE

Using the next generation matrix approach outlined in [36,37] to our model (1), the basic reproduction number can be computed by considering the below generation matrices F and V, that is, the Jacobian matrices associated to the rate of appearance of new infections and the net rate out of the corresponding compartments.

Matrix for the gain term, $F = \begin{pmatrix} \alpha S & \beta_1 & 0 & 0 \\ 0 & 0 & \gamma_1 & 0 \\ 0 & 0 & \varphi S & \delta \\ 0 & 0 & 0 & 0 \end{pmatrix}$, which implies $F = \begin{pmatrix} \alpha S_0 & \beta_1 & 0 & 0 \\ 0 & 0 & \gamma_1 & 0 \\ 0 & 0 & \varphi S_0 & \delta \\ 0 & 0 & 0 & 0 \end{pmatrix}$

at disease free equilibrium point.

Now, matrix for losses term, $V = \begin{pmatrix} (\beta_1+\beta_2+\gamma_3+\mu) & 0 & 0 & 0 \\ 0 & (\gamma_1+\mu) & 0 & 0 \\ 0 & 0 & (\delta+\psi_1+\psi_2+\mu) & 0 \\ 0 & 0 & 0 & (\lambda_1+\lambda_2+\mu) \end{pmatrix}$

which at disease free equilibrium point, becomes

$$V = \begin{pmatrix} (\beta_1+\beta_2+\gamma_3+\mu) & 0 & 0 & 0 \\ 0 & (\gamma_1+\mu) & 0 & 0 \\ 0 & 0 & (\delta+\psi_1+\psi_2+\mu) & 0 \\ 0 & 0 & 0 & (\lambda_1+\lambda_2+\mu) \end{pmatrix}.$$

Now we have to evaluate next generation matrix G,

Such that $G = FV^{-1}$

$$= \begin{pmatrix} \alpha S_0 & \beta_1 & 0 & 0 \\ 0 & 0 & \gamma_1 & 0 \\ 0 & 0 & \varphi S_0 & \delta \\ 0 & 0 & 0 & 0 \end{pmatrix} \begin{pmatrix} \frac{1}{(\beta_1+\beta_2+\gamma_3+\mu)} & 0 & 0 & 0 \\ 0 & \frac{1}{\gamma_1+\mu} & 0 & 0 \\ 0 & 0 & \frac{1}{(\delta+\psi_1+\psi_2+\mu)} & 0 \\ 0 & 0 & 0 & \frac{1}{(\lambda_1+\lambda_2+\mu)} \end{pmatrix}$$

$$= \begin{pmatrix} \frac{\alpha S_0}{(\beta_1+\beta_2+\gamma_3+\mu)} & 0 & 0 & 0 \\ 0 & 0 & 0 & 0 \\ 0 & 0 & \frac{\varphi S_0}{(\delta+\psi_1+\psi_2+\mu)} & 0 \\ 0 & 0 & 0 & 0 \end{pmatrix} \tag{6}$$

Table 1: Description and estimation of the parameters

Symbols	Descriptions	Values	Units
Δ	Recruitment rate of the susceptible individuals	0.0185	day^{-1}
α	Exposed rate of the individuals	0.152	day^{-1}
β_1	Effective rate of exposed becoming symptomatic individuals	0.138	Dimensionless
β_2	Effective rate of exposed becoming asymptomatic individuals	0.013	Dimensionless
γ_1	Probability of transmission of infection from symptomatic individuals	0.025	day^{-1}
γ_2	Probability of transmission of infection from asymptomatic individuals	0.015	day^{-1}
φ	Probability of transmission of infection from susceptible individuals	1.55	day^{-1}
γ_3	Quarantined rate from exposed individuals	0.25	Dimensionless
γ_4	Effective rate of quarantined individual becoming symptomatic individuals	0.02	day^{-1}
ρ	Effective rate of quarantined individual becoming susceptible individuals	0.025	day^{-1}
δ	Hospitalized rate of the infected individuals	0.4027	day^{-1}
λ_1	Death rate of the hospitalized individuals	0.0437	day^{-1}
λ_2	Rate of recovery from hospitalized individuals	0.8951	day^{-1}
ψ_1	Effective rate of recovery using self-immunity system	0.5887	day^{-1}
ψ_2	Death rate of the infected individuals	0.0418	day^{-1}
μ	Natural death rate	0.0078	day^{-1}

Hence, the largest eigen value of the matrix G is $\dfrac{\alpha\Delta}{\mu(\beta_1+\beta_2+\gamma_3+\mu)}$. Thus, the basic reproduction number of the model (1) is $R_0=\dfrac{\alpha\Delta}{\mu(\beta_1+\beta_2+\gamma_3+\mu)}$.

For the parameters used in our simulations (see Tab. 1), we compute this basic reproduction number to obtain $R_0=0.8724$.

4.5 Local Stability at Disease Free Equilibrium Point

Firstly, we investigate the local stability at disease free equilibrium point W_0. Before further proceeding, we need the following Theorem 3.

Theorem 3: The disease-free equilibrium of model (1) is locally asymptotically stable if $R_0<1$ and unstable if $R_0>1$.

Proof: To prove the Theorem 3, the following variation matrix [38] is computed corresponding to equilibrium point W_0. From the model (1), the Jacobean matrix of the model is

$$J=\begin{pmatrix} a_{11} & -\alpha S & 0 & \rho S & 0 & \varphi S & 0 & 0 & 0\\ aE & -(\beta_1+\beta_2+\gamma_3+\mu) & 0 & 0 & 0 & 0 & 0 & 0 & 0\\ 0 & \beta_1 & -(\gamma_1+\mu) & \gamma_4 & 0 & 0 & 0 & 0 & 0\\ 0 & \gamma_3 & 0 & -(\rho S+\gamma_4+\mu) & 0 & 0 & 0 & 0 & 0\\ 0 & \beta_2 & 0 & 0 & -(\gamma_2+\mu) & 0 & 0 & 0 & 0\\ 0 & 0 & \gamma_1 & 0 & \gamma_2 & a_{66} & 0 & 0 & 0\\ 0 & 0 & 0 & 0 & 0 & \delta & -(\lambda_1+\lambda_2+\mu) & 0 & 0\\ 0 & 0 & 0 & 0 & 0 & \psi_1 & \lambda_2 & -\mu & 0\\ 0 & 0 & 0 & 0 & 0 & \psi_2 & \lambda_1 & 0 & 0 \end{pmatrix} \tag{7}$$

where, $a_{11}=-(\alpha E+\varphi I+\mu)+\rho Q$ and $a_{66}=\varphi S-\delta-\psi_1-\psi_2-\mu$.

At disease free equilibrium, we get

$$J(W_0)=\begin{pmatrix} -\mu & -\alpha S_0 & 0 & \rho S_0 & 0 & \varphi S_0 & 0 & 0 & 0\\ 0 & -(\beta_1+\beta_2+\gamma_3+\mu) & 0 & 0 & 0 & 0 & 0 & 0 & 0\\ 0 & \beta_1 & -\gamma_1-\gamma_3-\mu & \gamma_4 & 0 & 0 & 0 & 0 & 0\\ 0 & 0 & \gamma_1 & -(\rho S_0+\gamma_4+\mu) & 0 & 0 & 0 & 0 & 0\\ 0 & 0 & 0 & 0 & -(\gamma_2+\mu) & 0 & 0 & 0 & 0\\ 0 & 0 & \gamma_1 & 0 & \gamma_2 & b_{66} & 0 & 0 & 0\\ 0 & 0 & 0 & 0 & 0 & \delta & -(\lambda_1+\lambda_2+\mu) & 0 & 0\\ 0 & 0 & 0 & 0 & 0 & \psi_1 & \lambda_2 & -\mu & 0\\ 0 & 0 & 0 & 0 & 0 & \psi_2 & \lambda_1 & 0 & 0 \end{pmatrix},$$

where $b_{66}=\varphi S_0-\delta-\psi_1-\psi_2-\mu$. In order to determine the stability of disease-free equilibrium point, we utilize $|J(W_0)-\lambda I|=0$, where λ be the eigen value and I be the identity matrix.

$$|J(W_0)-\lambda I|$$

$$=\begin{vmatrix} -\mu-\lambda & -\alpha S_0 & 0 & \rho S_0 & 0 & \varphi S_0 & 0 & 0 & 0 \\ 0 & b_{22}-\lambda & 0 & 0 & 0 & 0 & 0 & 0 & 0 \\ 0 & \beta_1 & b_{33}-\lambda & 0 & 0 & 0 & 0 & 0 & 0 \\ 0 & 0 & \gamma_1 & b_{44}-\lambda & \gamma_4 & 0 & 0 & 0 & 0 \\ 0 & 0 & 0 & 0 & -(\gamma_2+\mu)-\lambda & 0 & 0 & 0 & 0 \\ 0 & 0 & \gamma_1 & 0 & \gamma_2 & b_{66}-\lambda & 0 & 0 & 0 \\ 0 & 0 & 0 & 0 & 0 & \delta & -(\lambda_1+\lambda_2+\mu)-\lambda & 0 & 0 \\ 0 & 0 & 0 & 0 & 0 & \psi_1 & \lambda_2 & -\mu-\lambda & 0 \\ 0 & 0 & 0 & 0 & 0 & \psi_2 & \lambda_1 & 0 & 0 \end{vmatrix}=0,$$

where, $b_{22}=-(\beta_1+\beta_2+\gamma_3+\mu)$, $b_{33}=-\gamma_1-\gamma_3-\mu$ and $b_{44}=-(\rho S_0+\gamma_4+\mu)$.

By factoring out from the above matrix, we have

$$\lambda_1=-\mu<0,\quad \lambda_2=-\gamma_1-\mu<0,\quad \lambda_3=-(\rho S_0+\gamma_4+\mu)<0,\quad \lambda_4=-\gamma_2-\mu,$$
$$\lambda_5=-(\varphi S_0-\delta-\psi_1-\psi_2-\mu),\quad \lambda_6=-(\lambda_1+\lambda_2+\mu)<0,\quad \lambda_7=-\mu<0.$$

The remaining two eigen values can be obtained from this characteristic equation,

$$((\beta_1+\beta_2+\gamma_3+\mu)-\lambda)((\rho S_0+\gamma_3+\mu)-\lambda)=0.$$

After simplifying, the eigen values will be

$$\lambda=-((\beta_1+\beta_2+\gamma_3+\mu)+(\rho S_0+\gamma_3+\mu))\left(1-\frac{\alpha\Delta}{\mu(\beta_1+\beta_2+\gamma_3+\mu)}\right),$$

$$\therefore \lambda=-((\beta_1+\beta_2+\gamma_3+\mu)+(\rho S_0+\gamma_3+\mu))(1-R_0).$$

The eigenvalues of the equation are negative when $1-R_0>0$ i.e., $R_0<1$. Since all the eigen values are negative, the diseases free equilibrium point is locally stable when $R_0<1$.

This holds the Theorem 3.

4.6 Global Stability of the Disease-Free Equilibrium Point

In this section, we use the Lyapunov direct method [39,40] to show the conditions for the global asymptotic stability of the disease-free equilibrium point in int $(\mathbb{R}_9^+)$.

Theorem 4: The disease-free equilibrium point of the system (1) is globally asymptotically stable if $0<\frac{\delta+\psi_1}{\varphi}<R_0<1$ in the interior of the feasible region, otherwise it is unstable.

Proof: Theorem 4 can be proved based on the Lyapunov stability theorem [35,39]. For this purpose, we consider the following nonlinear Lyapunov function,

$$V = S - \overline{S} - \overline{S}\ln\frac{S}{\overline{S}} + E - \overline{E} - \overline{E}\ln\frac{E}{\overline{E}} + \frac{\rho\overline{I}}{\alpha\overline{E}}\overline{S}\left(I - \overline{I} - \overline{I}\ln\frac{I}{\overline{I}}\right) + \frac{\psi_2\overline{I}}{\mu}\overline{R}\left(R - \overline{R} - \overline{R}^2\ln\frac{R}{\overline{R}}\right).$$

Then V is C^1 on the interior of $\mathbb{R}_9^+$, $W_0\left(\overline{S},\overline{E},\overline{Q},\overline{M},\overline{A},\overline{I},\overline{H},\overline{R},\overline{D}\right)$ is the disease-free equilibrium point.

The derivative of V along the solution curves of (1) is given by the expression:

$$\dot{V} = \dot{S} - \frac{\overline{S}\dot{S}}{S} + \dot{E} - \frac{\overline{E}\dot{E}}{E} + \frac{\rho\overline{I}}{\alpha\overline{E}}\overline{S}\left(\dot{I} - \frac{\overline{I}}{I}\dot{I}\right) + \frac{\psi_2\overline{I}}{\mu}\overline{R}\left(\dot{R} - 2\overline{R}\frac{\overline{R}\dot{R}}{R}\right)$$

$$= \Delta + \rho SQ - (\alpha E + \varphi I)S - \mu S - \frac{\overline{S}}{S}[\Delta + \rho SQ - (\alpha E + \varphi I)S - \mu S] + \alpha SE - (\beta_1 + \beta_2 + \gamma_3)E - \mu E$$
$$- \frac{\overline{E}}{E}[\alpha SE - (\beta_1 + \beta_2 + \gamma_3)E - \mu E] + \frac{\rho S^* I^*}{\alpha\overline{E}}[\gamma_1 M + \gamma_2 A + \varphi SI - (\delta + \psi_1 + \psi_2)I - \mu I] - \frac{\overline{I}}{I}$$
$$[\gamma_1 M + \gamma_2 A + \varphi SI - (\delta + \psi_1 + \psi_2)I - \mu I] + \frac{\psi_1\overline{I}}{\mu}\overline{R}\left(\lambda_2 H + \psi_1 I - \mu R - R^*\frac{R^*}{R}[\lambda_2 H + \psi_1 I - \mu R]\right)$$

$$= \Delta\left(1 - \frac{\overline{S}}{S}\right) - \mu S\left(1 - \frac{\overline{S}}{S}\right) - (\alpha E + \varphi I)S\left(1 - \frac{\overline{S}}{S}\right) + \alpha SE\left(1 - \frac{\overline{E}}{E}\right) - (\beta_1 + \beta_2 + \gamma_3)E - \mu E\left(1 - \frac{\overline{E}}{E}\right)$$
$$- \mu I\frac{\rho\overline{S}}{\alpha\overline{E}} - \mu R\frac{\psi_2 I}{\mu}\left(1 - \frac{R}{R}\right) + \varphi SI\frac{\varphi I}{\alpha\overline{E}}\left(1 - \frac{\overline{I}}{I}\right) - (\delta + \psi_1 + \psi_2)I\frac{\varphi S}{\alpha E}\left(1 - \frac{\overline{I}}{I}\right)$$
$$+ (\lambda_2 H + \psi_1 I - \mu R)\frac{\psi_1 I}{\mu} + \phi(Q, M, A, H)$$

At the disease-free equilibrium point, putting $\Delta = \mu\overline{S}$ and simplifying the above equation, we get

$$\dot{V} = \mu\overline{S}\left(1 - \frac{\overline{S}}{S}\right) - \mu S\left(1 - \frac{\overline{S}}{S}\right) - (\alpha E + \varphi I)S\left(1 - \frac{\overline{S}}{S}\right) + \alpha SE - (\beta_1 + \beta_2 + \gamma_3)E - \mu E$$
$$- \mu I\frac{\rho\overline{S}}{\alpha}\mu R\frac{\psi_2 I}{\mu}R - \left(1 - \frac{\delta + \psi_1}{\varphi} - \frac{\alpha\Delta}{\mu(\beta_1 + \beta_2 + \gamma_3 + \mu)}\right)I\frac{\varphi S}{\alpha E}\frac{\psi_1 I}{\mu} + \phi(Q, M, A, H)$$
$$= \mu\overline{S}\left(1 - \frac{\overline{S}}{S}\right) - \mu S\left(1 - \frac{\overline{S}}{S}\right) - (\alpha E + \varphi I)S\left(1 - \frac{\overline{S}}{S}\right) + \alpha SE - (\beta_1 + \beta_2 + \gamma_3)E - \mu E$$
$$- \mu I\frac{\rho\overline{S}}{\alpha}\mu R\frac{\psi_2 I}{\mu}R - \left(1 - \frac{\delta + \psi_1}{\varphi} - R_0\right)I\frac{\varphi S}{\alpha E}\frac{\psi_1 I}{\mu} + \phi(Q, M, A, H).$$

Since all the parameter values and state variables are nonnegative, it follows that $\dot{V} \leq 0$ for $0 < \frac{\delta + \psi_1}{\varphi} < R_0 < 1$ with $\overline{V} = 0$ if and only if $S = \overline{S}$, $E = \overline{E}$, $Q = \overline{Q}$, $I = \overline{I}$, $R = \overline{R} = 0$ holds.

Thus, we can say that the disease-free equilibrium point is globally asymptotically stable when $0 < \frac{\delta + \psi_1}{\varphi} < R_0 < 1$.

This holds the Theorem 4.

4.7 Endemic Equilibrium Point (EEP)

Endemic equilibrium point (EEP) of the model (1) can be obtained by setting

$$\frac{dS}{dt} = 0, \quad \frac{dE}{dt} = 0, \quad \frac{dQ}{dt} = 0, \quad \frac{dM}{dt} = 0, \quad \frac{dA}{dt} = 0, \quad \frac{dI}{dt} = 0, \quad \frac{dH}{dt} = 0 \quad \text{and} \quad \frac{dR}{dt} = 0 \tag{8}$$

The differential equation for the death compartment ($D(t)$) is not present here. This is due to the fact that the state variable $D(t)$ only appears in the corresponding differential equation and so it has no significance in the overall system. Also, the number of death individuals at each instant t can be obtained from $N(t) = S(t) + E(t) + Q(t) + M(t) + A(t) + I(t) + H(t) + R(t) + D(t)$.

Let $W^*(S^*, E^*, Q^*, M^*, A^*, I^*, H^*, R^*)$ be the endemic equilibrium point and by solving the system (8), we get

$$W^*\left(S^*, E^*, Q^*, M^*, A^*, I^*, H^*, R^*, D^*\right) = \left(\frac{\beta_1 + \beta_2 + \gamma_3 + \mu}{a}, \frac{(\rho S^* + \gamma_4 + \mu) Q^*}{\gamma_3}, \frac{\beta_1 E^* + \gamma_4 Q^*}{\gamma_1 + \mu}, \frac{\gamma_3 E^*}{\rho S^* + \gamma_4 + \mu}, \frac{\beta_2 E^*}{\gamma_2 + \mu}, \frac{\gamma_1 M^* + \gamma_2 A^*}{\delta + \psi_1 + \psi_2 + \mu - \varphi S^*}, \frac{\delta I^*}{\lambda_1 + \lambda_2 + \mu}, \frac{\lambda_2 H^* + \psi_1 I^*}{\mu}\right)$$

where, $S^* = \frac{\beta_1 + \beta_2 + \gamma_3 + \mu}{\alpha}$, $E^* = \frac{\left(\beta_1 \mu - \alpha\Delta + \beta_2 \mu + \gamma_3 \mu + \mu^2\right) A_1}{\alpha A_2 (\beta_1 + \beta_2 + \gamma_3 + \mu)}$, $Q^* = \frac{(\beta_1 + \mu) A_3 A_4}{\rho A_5 (\gamma_4 + \mu)}$,

$M^* = \frac{\gamma_4 A_3 A_4}{\rho (\gamma_4 + \mu) A_5}$, $A^* = \frac{\beta_2 A_0 A_1}{\alpha (\beta_1 + \beta_2 + \gamma_3 + \mu) A_2 A_5}$, $I^* = \frac{\gamma_1 \gamma_4 A_3}{(\gamma_4 + \mu) A_5}$,

$H^* = \frac{\gamma_1 \gamma_4 (\delta + \psi_2) A_3}{(\gamma_4 + \mu)(\lambda_2 + \mu) A_5}$, $R^* = \frac{(\gamma_1 + \gamma_4) A_3}{\mu (\gamma_4 + \mu) A_5}$, such that $A_0 = \left(\alpha\Delta - \beta_1 \mu - \beta_2 \mu - \gamma_3 \mu - \mu^2\right)$,

$$A_1 = \left(\alpha\gamma^4 + \alpha\mu + \beta_1\rho + \gamma_3\rho + \mu\rho\right)\left(\alpha\mu^3 - \mu^3\varphi + \alpha\mu^2\psi_1 + \alpha\mu^2\psi_2 + \gamma_1\mu^2\varphi - \gamma_2\mu^2\varphi - \gamma_3\mu^2\varphi\right),$$

$$A_2 = \left(\alpha^2\mu^4 + \alpha\mu^4\rho - \mu^4\varphi\rho + \alpha^2\delta\mu^3 + \alpha^2\varphi\mu^3 + \alpha^2\psi_2 - \alpha\mu^4\rho - \alpha\beta_1\mu^3\varphi - \alpha\beta_2\mu^3\varphi + \alpha\beta_1\mu^3\rho - \alpha\gamma_3\right),$$

$$A_3 = \left(\mu^2 + \gamma_4\mu + \Delta\rho\right), \quad A_4 = (\delta\rho + \gamma_4\varphi + \mu\varphi + \mu\rho + \rho\psi_2),$$

$$A_5 = \left(\mu^2\varphi + \mu^2\rho + \delta\mu\rho + \gamma_1\mu\varphi + \gamma_4\mu\varphi\right).$$

4.8 Basic Reproduction Number at EEP

By applying the similar approach as given in Sub-section 4.4.1, we have basic reproduction number at the EEP.

Here, we get matrix for the gain term, $J_F = \begin{pmatrix} \alpha S^* & \beta_1 & 0 & 0 \\ 0 & 0 & \gamma_1 & 0 \\ 0 & 0 & \varphi S^* & \delta \\ 0 & 0 & 0 & 0 \end{pmatrix}$,

and matrix for losses term, $J_V = \begin{pmatrix} (\beta_1+\beta_2+\gamma_3+\mu) & 0 & 0 & 0 \\ 0 & (\gamma_1+\mu) & 0 & 0 \\ 0 & 0 & (\delta+\psi_1+\psi_2+\mu) & 0 \\ 0 & 0 & 0 & (\lambda_1+\lambda_2+\mu) \end{pmatrix}$.

Also, the next generation matrix, $G = J_F J_V^{-1}$

$$\therefore G = \begin{pmatrix} \dfrac{\alpha S^*}{(\beta_1+\beta_2+\gamma_3+\mu)} & 0 & 0 & 0 \\ 0 & 0 & 0 & 0 \\ 0 & 0 & \dfrac{\varphi S^*}{(\delta+\psi_1+\psi_2+\mu)} & 0 \\ 0 & 0 & 0 & 0 \end{pmatrix}.$$

Hence, the largest eigen value of the matrix G is $\dfrac{\varphi S^*}{(\delta+\psi_1+\psi_2+\mu)}$. Thus the basic reproduction number at EEP is $R_0^* = \dfrac{\varphi S^*}{(\delta+\psi_1+\psi_2+\mu)}$ where, $S^* = \dfrac{\beta_1+\beta_2+\gamma_3+\mu}{\alpha}$.

For the parameters used in our simulations (Tab. 1), it is easy to compute this basic reproduction number as $R_0^* = 4.0190$. This means that the pandemic outbreak has not been controlled in the world.

4.9 Local Stability at the Endemic Equilibrium Point

Theorem 5: The endemic equilibrium point of the model (1) is locally asymptotically stable if $R_0 > 1$ otherwise, it is unstable.

Proof: To determine the local stability at endemic equilibrium point, the characteristic equation of the model (1) is

$$\therefore |J(W)-\lambda I|$$

$$=\begin{vmatrix} b_{11}-\lambda & -\alpha S^* & 0 & \rho S^* & 0 & \varphi S^* & 0 & 0 & 0 \\ aE^* & -b_{22}-\lambda & 0 & 0 & 0 & 0 & 0 & 0 & 0 \\ 0 & \beta_1 & -(\gamma_1+\mu)-\lambda & \gamma_4 & 0 & 0 & 0 & 0 & 0 \\ 0 & \gamma_3 & 0 & -b_{44}-\lambda & 0 & 0 & 0 & 0 & 0 \\ 0 & \beta_2 & 0 & 0 & -(\gamma_2+\mu)-\lambda & 0 & 0 & 0 & 0 \\ 0 & 0 & \gamma_1 & 0 & \gamma_2 & b_{66}-\lambda & 0 & 0 & 0 \\ 0 & 0 & 0 & 0 & 0 & \delta & -b_{77}-\lambda & 0 & 0 \\ 0 & 0 & 0 & 0 & 0 & \psi_1 & \lambda_2 & -\mu-\lambda & 0 \\ 0 & 0 & 0 & 0 & 0 & \psi_2 & \lambda_1 & 0 & 0-\lambda \end{vmatrix} = 0,$$

here $b_{11} = -(\alpha E^* + \varphi I^* + \mu) + \rho Q^*$, $b_{22} = \beta_1 + \beta_2 + \gamma_3 + \mu$, $b_{44} = \rho S^* + \gamma_4 + \mu$, $b_{66} = \varphi S^* - \delta - \psi_1 - \psi_2 - \mu$ and $b_{77} = \lambda_1 + \lambda_2 + \mu$.

Therefore, the eigenvalues are

$$\lambda_1 = -\left(\alpha E^* + \varphi I^* + \mu\right) + \rho Q^*, \quad \lambda_2 = \frac{a\alpha S^* E^* - b_{11} b_{22}}{b_{11}}, \quad \lambda_3 = -\gamma_1 - \mu < 0,$$

$$\lambda_4 = \frac{a\rho\gamma_3 S^* E^* - a\alpha b_{44} S^* E^* + b_{11} b_{22} b_{44}}{a\alpha S^* E^* - b_{11} b_{22}}, \quad \lambda_5 = -\gamma_2 - \mu,$$

$$\lambda_6 = \frac{1}{h_1}\left(-a\varphi\mu\gamma_1\gamma_3\gamma_4 S^* E^* + h_2 S^* E^* - h_3 S^* E^* - h_4 S^* E^* + h_5\right), \quad \lambda_7 = -\left(\lambda_1 + \lambda_2 + \mu\right),$$

$$\lambda_8 = -\mu \quad \text{and} \quad \lambda_9 < 0, \text{ where, } h_1 = (\gamma_1 + \mu)\left(\alpha - a\alpha b_{44} S^* E^* + b_{11} b_{22} b_{44}\right)(\gamma_2 + \mu),$$

$$h_2 = a\rho\gamma_3 b_{66}\left(\mu\gamma_2 + \gamma_1\gamma_2 + \mu^2 + \mu\gamma_1\right), \quad h_3 = a\alpha\left(\mu\gamma_2 + \mu^2 + \mu\gamma_1\right),$$

$$h_4 = a\varphi\left((\mu\gamma_1 + \gamma_1\gamma_2) + \gamma_1\gamma_2\gamma_3\gamma_4\right) b_{44}, \quad h_5 = b_{11} b_{22} b_{44} b_{66}\left(\mu\gamma_2 + \gamma_1\gamma_2 + \mu\gamma_1 + \mu^2\right).$$

In this case, the basic reproduction number is more than one, i.e., $R_0 > 1$ according to the given data. Therefore, the endemic equilibrium point of the model (1) is locally asymptotically stable, which proves the Theorem 5.

4.10 Global Stability of the Endemic Equilibrium Point

In this section, we use the Lyapunov direct method to establish sufficient conditions for the global asymptotic stability of the endemic equilibrium point W^* in $\text{int}\left(\mathbb{R}_9^+\right)$ when $R_0 > 1$.

Theorem 6: The endemic equilibrium point W^* of the system (1) is globally asymptotically stable if $R_0 > 1$ in the interior of the feasible region, otherwise it is unstable.

Proof: Theorem 6 can be proved based on the Lyapunov stability theorem [21,39]. For that purpose, we consider the following nonlinear Lyapunov function,

$$L = S - S^* - S^* \ln\frac{S}{S^*} + E - E^* - E^* \ln\frac{E}{E^*} + \frac{\varphi S^* I^*}{\alpha E^*}\left(I - I^* - I^* \ln\frac{I}{I^*}\right) + \frac{\psi_1 I^* R^*}{\mu}\left(R - R^* - R^* \ln\frac{R}{R^*}\right) \tag{9}$$

Then L is C^1 on the interior of $\mathbb{R}_9^+$, W^* is the endemic equilibrium point.

The derivative of (9) along the solution curves of (1) is given by the expression:

$$\dot{L}=\dot{S}-\frac{S^*\dot{S}}{S}+\dot{E}-\frac{E^*\dot{E}}{E}+\frac{\varphi S^*I^*}{\alpha E^*}\left(\dot{I}-\frac{I^*\dot{I}}{I}\right)+\frac{\psi_1 I^*R^*}{\mu}\left(\dot{R}-R^*\frac{R^*\dot{R}}{R}\right)$$

$$=\Delta+\rho SQ-(\alpha E+\varphi I)S-\mu S-\frac{S^*}{S}\left[\Delta+\rho SQ-(\alpha E+\varphi I)S-\mu S\right]+\alpha SE-(\beta_1+\beta_2+\gamma_3)E$$

$$-\mu E-\frac{E^*}{E}\left[\alpha SE-(\beta_1+\beta_2+\gamma_3)E-\mu E\right]+\frac{\varphi S^*I^*}{\alpha E^*}\left[\gamma_1 M+\gamma_2 A+\varphi SI-(\delta+\psi_1+\psi_2)I-\mu I\right]-\frac{\overline{I}}{I}$$

$$\left[\gamma_1 M+\gamma_2 A+\varphi SI-(\delta+\psi_1+\psi_2)I-\mu I\right]+\frac{\psi_1 I^*R^*}{\mu}\left(\lambda_2 H+\psi_1 I-\mu R-R^*\frac{R^*}{R}\left[\lambda_2 H+\psi_1 I-\mu R\right]\right)$$

$$=\Delta\left(1-\frac{S^*}{S}\right)-\mu S\left(1-\frac{S^*}{S}\right)-(\alpha E+\varphi I)S\left(1-\frac{S^*}{S}\right)+\alpha SE\left(1-\frac{E^*}{E}\right)-(\beta_1+\beta_2+\gamma_3)E\left(1-\frac{E^*}{E}\right)$$

$$-\mu E\left(1-\frac{E^*}{E}\right)-\mu I\frac{\varphi S^*I^*}{\alpha E^*}\left(1-\frac{I^*}{I}\right)-\mu R\frac{\psi_1 I^*R^*}{\mu}\left(1-\frac{R^*}{R}\right)+\varphi SI\frac{\varphi S^*I^*}{\alpha E^*}\left(1-\frac{I^*}{I}\right)$$

$$-(\delta+\psi_1+\psi_2)I\frac{\varphi S^*I^*}{\alpha E^*}\left(1-\frac{I^*}{I}\right)+(\lambda_2 H+\psi_1 I-\mu R)\frac{\psi_1 I^*R^*}{\mu}\left(1-\frac{R^*}{R}\right)+\phi(Q,M,A,H) \tag{10}$$

At the endemic equilibrium point W^*, we have

$$\Delta=\left(\alpha E^*+\varphi I^*\right)S^*+\mu S^*-\rho S^*Q^*, \tag{11}$$

$$\beta_1+\beta_2+\gamma_3=\frac{\alpha SE^*-\mu E^*}{E^*}, \tag{12}$$

$$\delta+\psi_1+\psi_2=\frac{\gamma_1 M+\gamma_2 A+\varphi S^*I^*-\mu I^*}{I^*}. \tag{13}$$

Using the Eqs. (11)–(13) in (10), we obtain

$$\dot{L}=\left(\left(\alpha E^*+\varphi I^*\right)S^*+\mu S^*-\rho S^*Q^*\right)\left(1-\frac{S^*}{S}\right)-\mu S\left(1-\frac{S^*}{S}\right)-(\alpha E+\varphi I)S\left(1-\frac{S^*}{S}\right)$$

$$+\alpha SE\left(1-\frac{E^*}{E}\right)-\frac{\alpha SE^*-\mu E^*}{E^*}E\left(1-\frac{E^*}{E}\right)-\mu E\left(1-\frac{E^*}{E}\right)-\mu I\frac{\varphi S^*I^*}{\alpha E^*}\left(1-\frac{I^*}{I}\right)$$

$$-\mu R\frac{\psi_1 I^*R^*}{\mu}\left(1-\frac{R^*}{R}\right)+\varphi SI\frac{\varphi S^*I^*}{\alpha E^*}\left(1-\frac{I^*}{I}\right)-\frac{\gamma_1 M+\gamma_2 A+\varphi S^*I^*-\mu I^*}{I^*}I\frac{\varphi S^*I^*}{\alpha E^*}\left(1-\frac{I^*}{I}\right)$$

$$+(\lambda_2 H+\psi_1 I-\mu R)\frac{\psi_1 I^*R^*}{\mu}\left(1-\frac{R^*}{R}\right)+\phi(Q,M,A,H)$$

$$=\mu S^*\left(2-\frac{S^*}{S}-\frac{S}{S^*}\right)+(\alpha E+\varphi I)S^{*^2}+\rho S^*Q^*\left(1-\frac{S^*}{S}\right)\left(1-\frac{E^*}{E}\right)+\varphi SI\frac{\varphi S^*I^*}{\alpha E^*}\left(4-\frac{S^*}{S}-\frac{EI^*}{E^*I}-\frac{SR^*I}{S^*RI^*}\right)$$
$$\mu R\frac{\psi_1 I^*R^*}{\mu}\left(4-\frac{I^*}{I}-\frac{{\gamma_1}^2S^{*^2}I^{*^2}}{I}-\frac{I^{*^2}R^{*^3}}{R^2}\right)-\frac{\mu\varphi S^*I^*I^2}{\alpha E^*}\left(1-\frac{I^{*2}}{I^2}\right)+\frac{\psi_1\varphi S^*I^{*2}R^*}{\alpha\mu E^*}+\phi(Q,M,A,H)$$

$$=\mu S^*\left(2-\frac{S^*}{S}-\frac{S}{S^*}\right)+(\alpha E+\varphi I)S^{*^2}+\varphi SI\frac{\varphi S^*I^*}{\alpha E^*}\frac{{\gamma_1}^2S^{*^2}I^{*^2}}{I^*}\mu R\frac{\psi_1 I^*R^*}{\mu}\left(4-\frac{S^*}{S}-\frac{EI^*}{E^*I}-\frac{RE^*}{R^*E}-\frac{SR^*I}{S^*RI^*}\right)$$
$$-\rho S^*Q^*\left(1-\frac{S^*}{S}\right)\left(1-\frac{E^*}{E}\right)\frac{\mu\varphi S^*I^*}{\alpha E^*}\left(\frac{\Delta\varphi}{\mu(\delta+\psi_1+\psi_2+\mu)}-1\right)+\phi(Q,M,A,H)$$

$$=\mu S^*\left(2-\frac{S^*}{S}-\frac{S}{S^*}\right)+(\alpha E+\varphi I)S^{*^2}+\varphi SI\frac{\varphi S^*I^*}{\alpha E^*}\frac{{\gamma_1}^2S^{*^2}I^{*^2}}{I^*}\mu R\frac{\psi_1 I^*R^*}{\mu}\left(4-\frac{S^*}{S}-\frac{EI^*}{E^*I}-\frac{RE^*}{R^*E}-\frac{SR^*I}{S^*RI^*}\right)$$
$$-\rho S^*Q^*\left(1-\frac{S^*}{S}\right)\left(1-\frac{E^*}{E}\right)\frac{\mu\varphi S^*I^*}{\alpha E^*}(R_0-1)+\phi(Q,M,A,H).$$

Since the arithmetic mean is greater than or equal to the geometric mean, it follows that

$$2-\frac{S^*}{S}-\frac{S}{S^*}\le 0,$$
$$4-\frac{S^*}{S}-\frac{EI^*}{E^*I}-\frac{RE^*}{R^*E}-\frac{SR^*I}{S^*RI^*}\le 0,$$

Further, since all the parameters of the model are nonnegative, it follows that $\dot{L}\le 0$ for $R_0>1$ with $\dot{L}=0$ if and only if $S=S^*$, $E=E^*$, $Q=Q^*$, $M=M^*$, $A=A^*$, $I=I^*$, $H=H^*$, $R=R^*$ and $D=D^*$ holds.

The largest compact invariant set in $\left\{(S,E,Q,M,A,I,H,R,D)\in\mathbb{R}_9^+: dL/dt=0\right\}$ is the singleton $\{W^*\}$, where W^* is the endemic equilibrium point. By LaSalle's invariance principle [41,42], it implies that W^* is globally asymptotically stable in the interior of $\mathbb{R}_9^+$.

Hence, the Theorem 6 is proved.

4.11 Sensitivity Analysis

In determining the best strategy to reduce the disease transmission and human mortality due to pandemic outbreak of COVID-19, it is necessary to know the relative importance of the different factors responsible for its transmission and prevalence. Initial disease transmission is directly related to R_0^*, and disease prevalence is directly related to the endemic equilibrium point. Sensitivity analysis is the study of how the uncertainty in the output of a mathematical model or system can be divided and allocated to different sources of uncertainty in its inputs. It tells us how important each parameter is to disease transmission. Such information is crucial not only for experimental design, but also to data assimilation and reduction of complex nonlinear models [43]. Sensitivity analysis is commonly used to determine the robustness of model predictions to parameter values, since there are usually errors in data collection and presumed parameter values. It is used to discover parameters that have a high impact on R_0^* and should be targeted by intervention strategies [44].

More accurately, sensitivity indices allow us to measure the relative change in a variable when a parameter changes. The normalized forward sensitivity index of a variable with respect to a parameter is the ratio of the relative change in the variable to the relative change in the parameter. When the variable is a differentiable function of the parameter, the sensitivity index may be alternatively defined using partial derivatives.

Definition 4.2: ([14]) The normalized forward sensitivity index of R_0^*, which is differentiable with respect to a given parameter P, is defined by

$$\gamma_P^{R_0^*} = \frac{\partial R_0^*}{\partial P}\frac{P}{R_0^*}$$

As we have an explicit formula for R_0^*, we derive an analytic expression for the sensitivity R_0^* to each of the different parameters described in Tab. 1. For example, the sensitivity index of R_0^* with respect to φ is

$$\gamma_\varphi^{R_0^*} = \frac{\partial R_0^*}{\partial \varphi}\frac{\varphi}{R_0^*} = 0.9973$$

These values have been calculated analytically from the real data collected from [30] (see also [13,15] for the sources of similar data) such that the mathematical model describes the present transmission scenario well. The description of all the parameters with the estimated values used in the simulations of model (1) is presented in Tab. 1.

The values of the sensitivity indices for the different parameters of Tab. 1 are presented in Tab. 2.

Table 2: Sensitivity indices of R_0^* evaluated for the parameter values given in Tab. 1

Parameters	Values	Sensitivity index
α	0.15	−0.7711
β_1	0.14	0.0515
β_2	0.01	0.0037
φ	1.55	0.9973
γ_3	0.25	0.0920
ψ_1	0.5887	−0.2214
ψ_2	0.0428	−0.0016
μ	0.0078	−0.0064

Note that, the sensitivity index may depend on several parameters of the system, but also can be constant, independent of any parameter. For example, $\gamma_P^{R_0^*} = +1$ means that increasing (decreasing) P by a given percentage increases (decreases) always R_0^* by that same percentage. The estimation of a sensitive parameter should be carefully done, since a small perturbation in such parameter leads to relevant quantitative changes. On the other hand, the estimation of a parameter with a rather small value for the sensitivity index does not require as much attention to estimate, because a small perturbation in that parameter leads to small changes. From Tab. 2, we

conclude that the most sensitive parameters to the basic reproduction number R_0^* of the COVID-19 model (1) are φ, α and ψ_1. In concrete, an increase of the value of φ will increase the basic reproduction number by 99.73%. In contrast, an increase of the value of α will decrease R_0^* by 77.11%.

5 Numerical Simulations

We perform numerical simulations to compare the results of our model with the real data published by Worldometer [30] till July 10, 2020. We show that our COVID-19 model describes well the real data of daily confirmed cases during the 2 months outbreak. The computational study for graphical representation of the model (1) was performed by ode45 solver using MATLAB programming language. We use a set of suitable parameter values as presented in Tab. 1 for the simulations. We have considered the initial condition $S_0 = 100 \times 10^5$, $E_0 = 70 \times 10^5$, $\mathrm{Q}_0 = 60 \times 10^5$, $M_0 = 40 \times 10^5$, $A_0 = 30 \times 10^5$, $\mathrm{I}_0 = 10 \times 10^5$, $H_0 = 7 \times 10^5$, $R_0 = 8 \times 10^5$ and $D_0 = 2 \times 10^4$. Firstly, we solve the model (1) considering the initial values and all other parameters that are shown in Tab. 1. Also, we have performed the numerical simulations for time interval $t \in [0, 60]$ for 60 days.

Our object is to study the effects of infection rate (φ) from susceptible individuals, probability of transmission of infection from symptomatic individuals (γ_1), probability of transmission of infection from asymptomatic individuals (γ_2), quarantined rate (γ_3) and effective rate of recovery using self-immunity system (ψ_1) in case of disease transmission. We have selected these parameters because they have a large impact in determining the best strategy to reduce the disease transmission and human mortality due to pandemic outbreak of COVID-19. So, if it is possible to minimize the infection rate from susceptible individuals, rate of transmission of infection from symptomatic individuals, rate of transmission of infection from asymptomatic individuals and maximize the quarantined rate and effective rate of recovery using self-immunity system then the spreading of novel coronavirus will be controlled.

Considering these parameters into account, we have run the program for the state variables to show all state trajectories simultaneously. The result of simulation of the combined class is presented in Fig. 4.

From Fig. 4, we observe that the susceptible and quarantined individuals are decreased monotonically. At the same time, the exposed individuals initially increase but after some days it gradually decreases. From the very beginning of this pandemic, the symptomatic curve is increased rapidly than asymptomatic individual but after some days asymptomatic curve is also increased surprisingly. However, a massive number of individuals having no symptoms of COVID-19 transmit the virus to others. Due to increase these symptomatic and asymptomatic individuals the infected individual increases extensively. As a result, hospitalized and death individuals are also increased than that of recovered individuals. From the dynamical behavior of the graph, it is anticipated that the infected individuals will continue to grow up with the passes of time until the initiation of vaccine or proper medicine. Though, it can be controlled by maintaining physical distances, increasing quarantined rate and developing self-immunity system which reflect our study.

Again, we run the program keeping all other values of the parameters same as before for the susceptible, infected and death individuals. The result of simulation in this case is presented in Fig. 5.

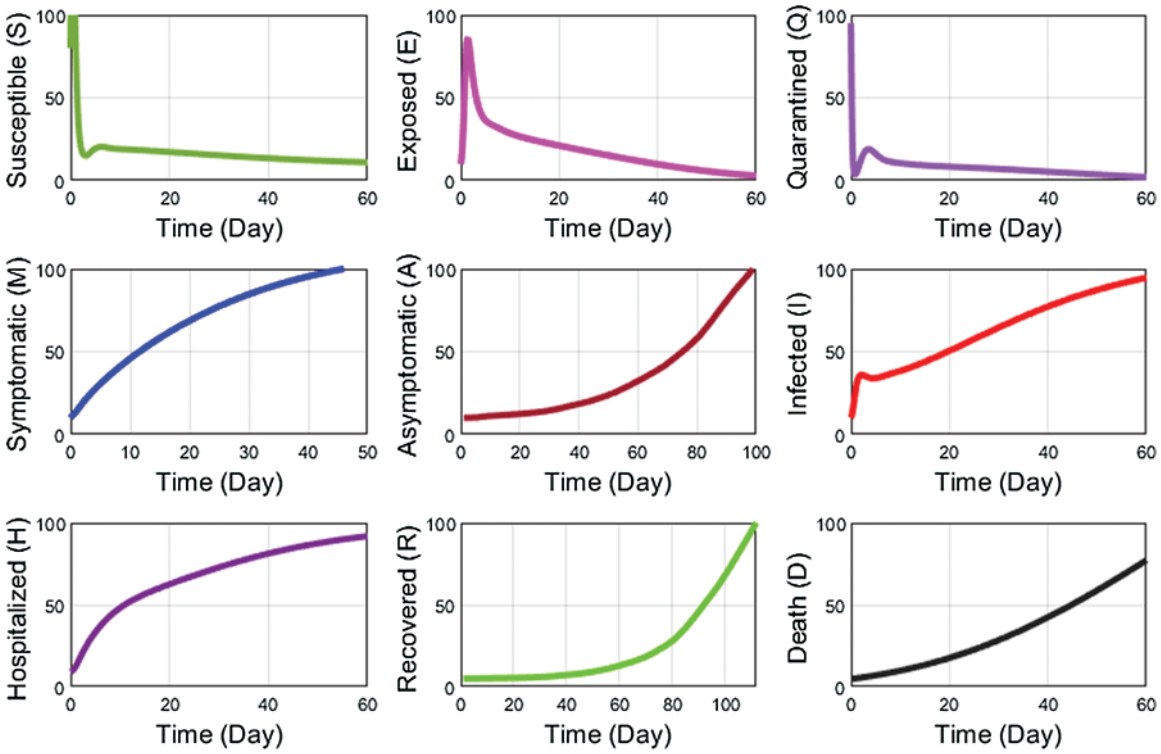

Figure 4: Simulations for the coronavirus infection of the population with time (60 days) when the basic reproduction number is greater than 1

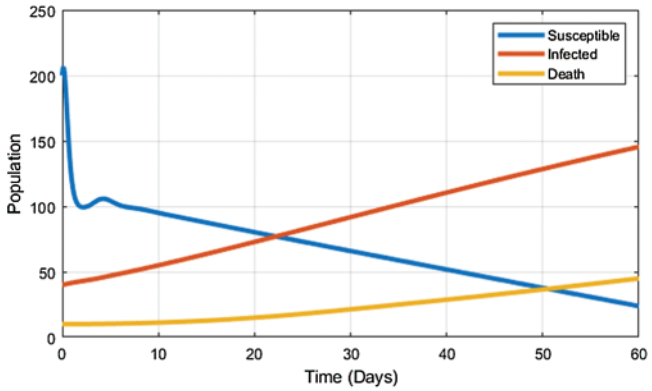

Figure 5: Dynamics of susceptible, Infected and Death individuals where the infected individuals increase significantly as a result the rate of death from coronavirus is increasing day by day

Fig. 5 shows the state trajectories of three compartments such as susceptible, infected and death individuals in the absence of any control measures. We have observed that the infected individuals increase sharply whereas the death individuals increase steadily from the initial state. Thus, these two individuals lead the susceptible individuals to be decreased dramatically.

Now, we run the program for the quarantined, infected and recovered individuals to show the effect of quarantine rate keeping the parameters value same as before. The result of simulation in this case is shown in Fig. 6.

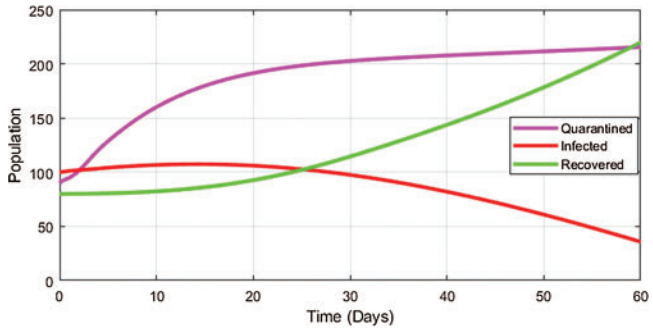

Figure 6: Dynamics of quarantined, infected and recovered individuals where recovered individuals are increased due to increase of quarantined individuals

In Fig. 6, we see the variation of three state trajectories of quarantined, infected and recovered individuals with time. It has been observed that the infected individuals decrease significantly as the quarantined rate increases. As a result, the decreasing rate of infected individuals bolsters the recovered individuals to be increased extensively.

We also observe from Fig. 7 that the infected populations are significantly decreased due to maintain the quarantine system strictly. The figure shows that if the quarantined rate is increased from $\gamma_3 = 0.25$ to $\gamma_3 = 0.50$, the probability to become COVID-19 positive is very little. In this case, the recovered individuals are also enhanced for the high rate of quarantine rate.

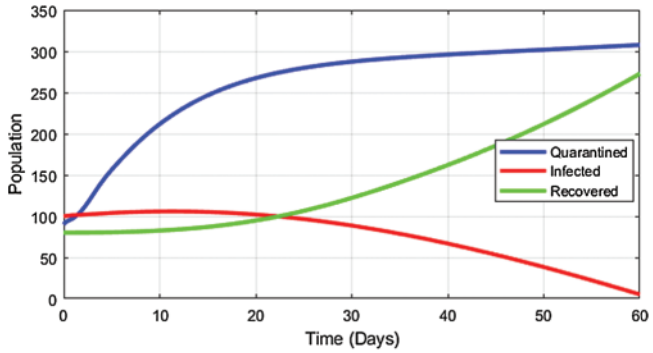

Figure 7: Dynamics of quarantined, infected and recovered individuals where the infected population is significantly decreased due to increase of quarantined rate from $\gamma_3 = 0.25$ to $\gamma_3 = 0.50$

Again, we solve the model numerically for the class asymptomatic and infected individuals to show how the change in the infected individuals due to impact of asymptomatic individuals. The result in this case is presented in Fig. 8.

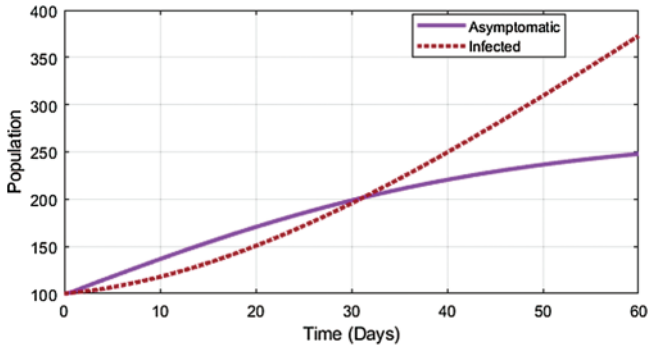

Figure 8: Dynamics of asymptomatic and infected individuals where the infected individuals are extensively increased due to increase of asymptomatic individuals

Fig. 8 represents the variation of asymptomatic and infected individuals with time while symptomatic and other effects are not considered. We observe that the infected population is extremely increased due to increase of asymptomatic individuals. Because an asymptomatic individual does not exhibit the symptoms of COVID-19 outbreak but can transmit the virus to others susceptible individuals and due to scarcity of symptoms the family members and others live together with him and they become COVID-positive in absence of mind and still transmit the virus to other members. Therefore, the population presenting no symptoms of the disease can transmit the coronavirus rapidly.

In Fig. 9, we notice that infected populations of COVID-19 are increased with the increase rate of symptomatic individuals. The important thing is that, the infected individuals are increased due to symptomatic individuals but not as like in asymptomatic case.

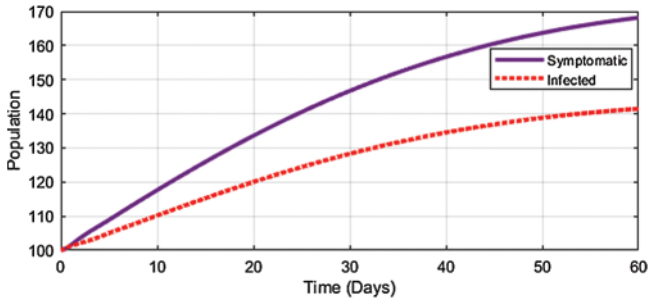

Figure 9: Dynamics of symptomatic and infected individuals where the infected population is increased but not tremendously due to increase of symptomatic population

Next, we solve the model for the class of infected individuals to show how the change in the infected individuals for different values of self-immunity rate. The result in this case is presented in Fig. 10.

From Fig. 10, it has been observed that the infected populations are decreased tremendously due to increase of self-immunity system (i.e., by increasing the self-immunity rate from $\psi_1 = 0.27$ to $= 0.37$). Hence, to reduce the infected individuals from this outbreak, self-immunity system must be developed for all the populations of a community. For that reason, it is mandatory for each of the individuals to develop a strong immune system through indoor and outdoor

activities, by trying muscle strength training, by eating a diet high in fruits, vegetables, and whole grains and to restrict saturated fats and sugars to 10% of total calories while minimizing the consumption of red and processed meats.

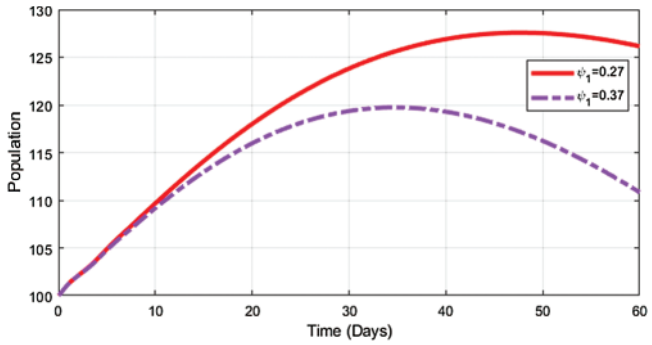

Figure 10: Variation of infected individuals for different values of self-immunity rate where the infected populations are significantly decreased due to increase of self-immunity system

In the epidemiology, disease transmission and disease prevalence are directly related to value of basic reproduction number and endemic equilibrium point. It provides an incursion formula for the initial spread of the disease in a susceptible population and it's defined as the average number of secondary infectious population that occurs when one infective people is introduced it into others susceptible population. It is cleared to define that the outbreak of corona virus infection will be eliminated if $R_0 < 1$ and remained in the community if $R_0 > 1$. Now, we run the program to know which parameters are responsible for the corona virus transmission by considering the initial values and parameters value that are shown in Tab. 1. The result obtained in this case is given in Figs. 11–14.

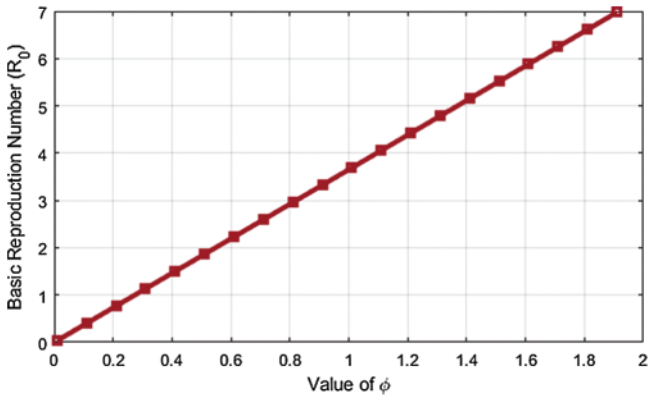

Figure 11: Numerical simulation of basic reproduction number with respect to the infectious rate φ, where the value of R_0 is increased linearly as the increase of φ, i.e., the disease persist in the community with the increase of infectious rate

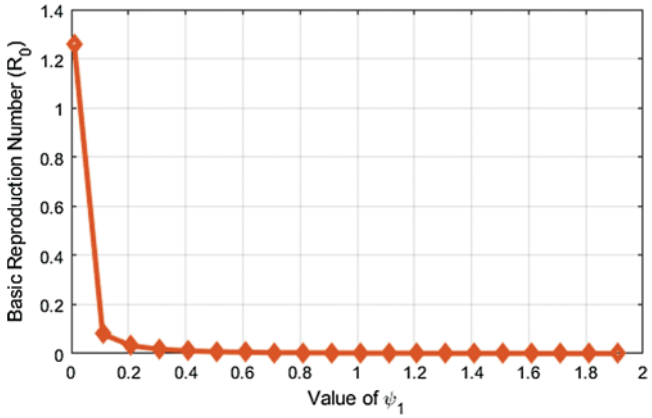

Figure 12: The value of R_0 is decreased with respect to the rate of self-immunity system ψ_1, and $R_0 < 1$ when $0.04 < \psi_1$

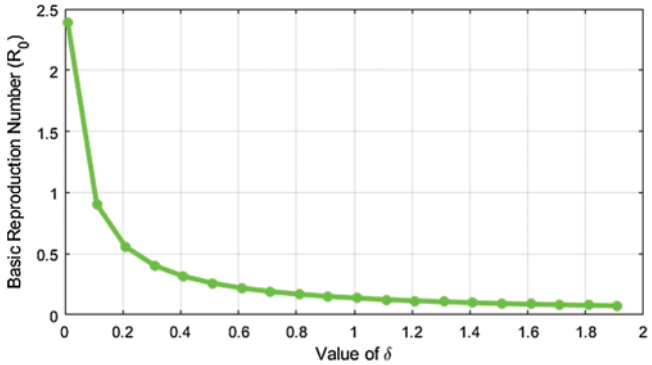

Figure 13: The value of R_0 is decreased significantly with respect to the increase of isolation rate, δ, and $R_0 < 1$, i.e., asymptotically stable in the region $0.1 < \psi_1$

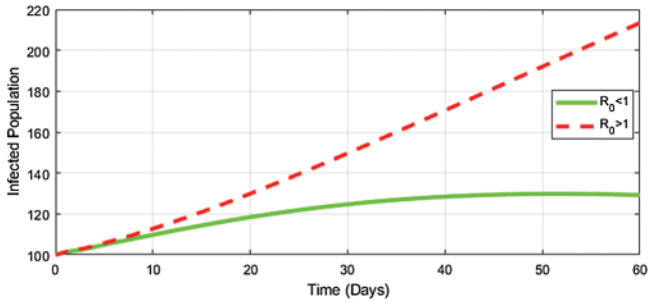

Figure 14: The overall stability of pandemic corona virus infection using the parameter values in Tab. 1, that may be wiped out when $R_0 < 1$ and persist in the community when $R_0 > 1$

Figs. 11–14 show the dynamics of the basic reproduction number with respect to the important parameters that are responsible to continue this pandemic situation. It is observed from Fig. 11 that the value of the basic reproduction number is increased linearly as the increase of

the value of infectious rate. In this case, the disease persists in the community. It is also clear from Figs. 12 and 13 that the value of basic reproduction number is extensively decreased with respect to the self-immunity system as well as the increase of isolation rate. Fig. 14 illustrates the overall scenario of the COVID-19 situation with respect to the basic reproduction number. The pandemic corona virus infection may be wiped out when $R_0 < 1$ and persist in the community when $R_0 > 1$. Thus, to eradicate the outbreak of coronavirus, it is important to develop the individuals' self-immunity system and maintain the physical distances strictly.

6 Conclusions

COVID-19 is a highly infectious pandemic disease which is impendence for the whole world. There is no specific treatment for this novel coronavirus disease which leads it more deadlier. This paper deals with a nine mutually exclusive compartmental model on transmission dynamics of COVID-19. The compartmental model has been investigated with mathematical analysis and computer simulations in order to understand the dynamics of this disease transmission. In our study, we have observed that the spread of novel coronavirus largely depends on the rate of close contact between susceptible and infected individuals. From Figs. 6 and 7, it has been observed that the death rate from coronavirus disease increases as the infection rate increases whereas infection rate extensively decreases with the increase of quarantined individuals. The quarantined individuals also lead to increase of recovered individuals. In Figs. 8 and 9, we have noticed that the infection rate of COVID-19 increases more surprisingly as the rate of asymptomatic individuals increases than that of the symptomatic individuals. Figs. 7 and 10 show that the infection rate significantly reduces due to increase of quarantined rate as well as the self-immunity rate. From the sensitivity analysis, we have obtained that the most sensitive parameters to the basic reproductive ratio of the COVID-19 model (1) are infection rate (φ), exposed rate (α) and the self-immunity rate (ψ_1). Our findings suggest that to combat or eradicate this pandemic outbreak, the physical distances must be maintained rigorously. It is also highly recommended for eating immune-boosting foods to increase immunity and taking immune-boosting drugs to defend the virus.

Authors' Contributions: This research is a group work carried out in collaboration among all authors. Authors MHAB and MAI designed the study, performed the conceptualization and methodological analysis and model formulation of the first draft of the manuscript. Authors SA and SM analyzed the model analytically and wrote some literature of the study. Author AKP wrote the programming codes and performed some part of the computational analysis. Author SAS contributed to literature searches and calculated the real data to estimate the parameters, MSK and MRK verified the parameters and checked the literature. All authors have read and agreed to publish the final version of the manuscript.

Data Availability: The data used to support the findings of this study are included within the article.

Funding Statement: The authors greatly acknowledge the partial financial support provided by the Ministry of Science and Technology, Government of the People's Republic of Bangladesh under special allocation in 2019–2020 with the research Grant Ref. No. 39.00.0000.009.06.024.19-12/410(EAS). Supports with Ref.: 17-392RG/MATHS/AS_I-FR3240297753 funded by TWAS,

Italy and Ref. No. 6(74) UGC/ST/Physical-17/2017/3169 funded by the UGC, Bangladesh are also acknowledged.

Conflicts of Interest: The authors declare that they have no conflicts of interest to report regarding the present study.

References

1. Harbeck, M., Seifert, L., Hänsch, S., Wagner, D. M., Birdsell, D. et al. (2013). Yersinia Pestis DNA from skeletal remains from the 6th century AD reveals insights into Justinian plague. *PLoS Pathogens, 9(5),* e1003349. DOI 10.1371/journal.ppat.1003349.
2. COVID-19: A History of Coronavirus (2020). https://www.labmanager.com/lab-health-and-safety/covid-19-a-history-of-coronavirus.
3. Prompetchara, E., Ketloy, C., Palaga, T. (2020). Immune responses in COVID-19 and potential vaccines: Lessons learned from SARS and MERS epidemic. *Asian Pacific Journal of Allergy and Immunology, 38(1),* 1–9. DOI 10.12932/AP-200220-0772.
4. Brauer, F., Castillo-Chavez, C., Feng, Z. (2019). *Mathematical models in epidemiology*. New York: Springer Verlag.
5. Biswas, M. H. A., Samad, S. A. (2020). Dynamical transmission of HIV/AIDS and TB co-infection model. *Proceedings of the International Conference on Industrial Engineering and Operations Management,* pp. 2261–2273, Dubai, UAE, 2020.
6. Biswas, M. H. A. (2012). Model and control strategy of the deadly Nipah Virus (NiV) infections in Bangladesh. *Research & Reviews in BioSciences, 6(12),* 370–377.
7. Khatun, M. S., Biswas, M. H. A. (2020). Mathematical analysis and optimal control applied to the treatment of leukemia. *Journal of Applied Mathematics and Computing, 64(1–2),* 331–353. DOI 10.1007/s12190-020-01357-0.
8. Khatun, M. S., Biswas, M. H. A. (2020). Optimal control strategies for preventing hepatitis B infection and reducing chronic liver cirrhosis incidence. *Infectious Disease Modelling, 5(2020),* 91–110. DOI 10.1016/j.idm.2019.12.006.
9. Khatun, M. S., Biswas, M. H. A. (2019). Modeling the effect of adoptive T cell therapy for the treatment of leukemia. *Computational and Mathematical Methods, 2(2),* 1545. DOI 10.1002/cmm4.1069.
10. Burges, D. N., Borrie, M. S. (1981). *Modeling with differential equations*. New York, USA: Ellis Horwood Limited.
11. Wu, J., Leung, K., Leung, G. M. (2020). Nowcasting and forecasting the potential domestic and international spread of the 2019-Ncov outbreak originating in Wuhan, China: A modelling study. *Lancet, 395(10225),* 689–697.
12. Zhang, J., Weili, W., Zhao, X., Zhang, W. (2020). Recommended psychological crisis intervention response to the 2019 novel coronavirus pneumonia outbreak in China: A model of West China hospital. *Precision Clinical Medicine, 3(1),* 3–8. DOI 10.1093/pcmedi/pbaa006.
13. Zhang, S., Diao, M., Yu, W., Pei, L., Lin, Z. et al. (2020). Estimation of the reproductive number of novel coronavirus (COVID-19) and the probable outbreak size on the diamond princess cruise ship: A data-driven analysis. *International Journal of Infectious Diseases, 93,* 201–214. DOI 10.1016/j.ijid.2020.02.033.
14. Ndairou, F., Area, I., Nieto, J. J., Torres, D. F. M. (2020). Mathematical modeling of COVID-19 transmission dynamics with a case study of Wuhan. *Chaos Solitons Fractals, 135,* 109846. DOI 10.1016/j.chaos.2020.109846.
15. Xu, X., Chen, P., Wang, J., Feng, J., Zhou, H. et al. (2020). Evolution of the novel coronavirus from the ongoing Wuhan outbreak and modeling of its spike protein for risk of human transmission. *Science China Life Sciences, 63(3),* 457–460. DOI 10.1007/s11427-020-1637-5.

16. Aguilar, J. B., Faust, G. S., Westafer, M. L. M., Gutierrez, J. B. (2020). Investigating the impact of asymptomatic carriers on COVID-19 transmission. *MedRxiv Preprint*. DOI 10.1101/2020.03.18.20037994.
17. Andrew, N. (2007). Contesting the cause and severity of the black death: A review essay. *International Institute for Applied Systems Analysis, 33(3),* 616–627.
18. Biswas, M. H. A., Paiva, L. T., de Pinho, M. D. R. (2014). A SEIR model for control of infectious diseases with constraints. *Mathematical Biosciences and Engineering, 11(4),* 761–784. DOI 10.3934/mbe.2014.11.761.
19. Biswas, M. H. A., Khatun, M. S., Paul, A. K., Khatun, M. R., Islam, M. A. et al. (2020). Modeling the effective control strategy for the transmission dynamics of global pandemic COVID-19. *Collection 'COVID-19 SARS-CoV-2.'* DOI 10.1101/2020.04.22.20076158.
20. Biswas, M. H. A. (2012). AIDS epidemic worldwide and the millennium development strategies: A light for lives. *HIV & AIDS Review, 11(4),* 87–94. DOI 10.1016/j.hivar.2012.08.004.
21. Buonomo, B., Vargas-De-León, C. (2012). Global stability for an HIV-1 infection model including an eclipse stage of infected cells. *Journal of Mathematical Analysis and Applications, 385(2),* 709–720. DOI 10.1016/j.jmaa.2011.07.006.
22. Latest Research on Asymptomatic Carriers (2020). https://www.businessinsider.com/coronavirus-carriers-transmit-without-symptoms.
23. Islam, M. A., Imran, M. B. U., Biswas, M. H. A. (2020). Modeling the effects of transmission dynamics of malaria: A mathematical approach on healthcare. *Proceedings of the International Conference on Industrial Engineering and Operations Management,* pp. 2191–2202. Dubai, UAE.
24. Islam, M. A., Biswas, M. H. A. (2019). Optimal planning and management of groundwater level declination: A mathematical model. *Proceedings of the 2nd International Conference on Industrial and Mechanical Engineering and Operations Management,* pp. 107–117. Dhaka, Bangladesh.
25. El Allaoui, A., Melliani, S., Chadli, L. S. (2020). A simple mathematical model for Coronavirus (COVID-19). In collection 'COVID-19 SARS-CoV-2,' preprints from medRxiv and bioRxiv. DOI 10.1101/2020.04.23.20076919.
26. Nadeem, S. (2020). Coronavirus COVID-19: Available free literature provided by various companies. *Journals and Organizations Around the World, 5(1),* 7–13.
27. Coronavirus Cases Rising Fast in Bangladesh (2020). https://en.prothomalo.com/bangladesh/coronavirus-cases-rising-fast-in-bangladesh.
28. Chen, N., Zhou, M., Dong, X., Zhang, L., Zhang, X. et al. (2020). Epidemiological and clinical characteristics of 99 cases of 2019 Novel Coronavirus pneumonia in Wuhan, China: A descriptive study. *Lancet, 395(10223),* 507–513. DOI 10.1016/S0140-6736(20)30211-7.
29. COVID-19-Spreads-Transmission (2020). https://www.livescience.com/how-covid-19-spreads-transmission.
30. COVID-19 Coronavirus Pandemic (2020). https://www.worldometers.info/coronavirus/.
31. COVID-19 Situation Update for the EU (2020). https://www.ecdc.europa.eu/en/cases-2019-ncov-eueea.
32. UNDP Report, COVID-19 Pandemic in America (2020). https://www.undp.org/content/undp/en/home/news-centre/news/2020/LAC_COVID19.
33. World Bank Report, COVID-19 in South Asia (2020). https://www.worldbank.org/en/region/sar/overview.
34. WHO African Region, External Situation Report 01 (2020). https://apps.who.int/iris/handle/10665/331330.
35. Number of COVID-19 Cases per 100,000 Population in Australia and Oceania (2020). https://www.statista.com/map/australia-and-oceania.
36. Driessche, P. V. D., Watmough, J. (2002). Reproduction numbers and sub-threshold endemic equilibria for compartmental models of disease transmission. *Mathematical Biosciences, 180(1–2),* 29–48. DOI 10.1016/S0025-5564(02)00108-6.
37. Heffernan, J. M., Smith, R. J., Wahl, L. M. (2005). Perspectives on the basic reproductive ratio. *Journal of the Royal Society Interface, 2(4),* 281–293. DOI 10.1098/rsif.2005.0042.

38. Gantmacher, F. R. (1998). *The theory of matrices,* vol. 1. Providence, RI: AMS Chelsea Publishing.
39. Huo, H. F., Feng, L. X. (2012). Global stability of an epidemic model with incomplete treatment and vaccination. *Discrete Dynamics in Nature and Society, 2012(530267),* 1–14. DOI 10.1155/2012/530267.
40. Vargas-De-Leon, C. (2017). Global stability of infectious disease models with contact rate as a function of prevalence index. *Mathematical Biosciences and Engineering, 14(4),* 1019–1033. DOI 10.3934/mbe.2017053.
41. Cheng, Y., Wang, J., Yang, X. (2012). On the global stability of a generalized cholera epidemiological model. *Journal of Biological Dynamics, 6(2),* 1088–1104. DOI 10.1080/17513758.2012.728635.
42. Safi, M. A., Garba, S. M. (2012). Global stability analysis of SEIR model with holling type II incidence function. *Computational and Mathematical Methods in Medicine, 2012(826052),* 1–8. DOI 10.1155/2012/826052.
43. Chitnis, N., Hyman, J. M., Cushing, J. M. (2008). Determining important parameters in the spread of malaria through the sensitivity analysis of a mathematical model. *Bulletin of Mathematical Biology, 70(5),* 1272–1296. DOI 10.1007/s11538-008-9299-0.
44. Rodrigues, H. S., Monteiro, M. T. T., Torres, D. F. M. (2013). Sensitivity analysis in a dengue epidemiological model. *Conference Papers in Mathematics, 2013*. DOI 10.1155/2013/721406.